BIOCHEMISTRY
including biophysical chemistry & molecular biology

Article

pubs.acs.org/biochemistry

Protonated Rhodosemiquinone at the Q_B Binding Site of the M265IT Mutant Reaction Center of Photosynthetic Bacterium *Rhodobacter sphaeroides*

Ágnes Maróti,[†] Colin A. Wraight,[†,§] and Péter Maróti*[,‡]

[†]Department of Pediatrics and [‡]Department of Medical Physics, University of Szeged, Szeged, Hungary H-6720

[§]Center for Biophysics and Computational Biology and Department of Plant Biology, University of Illinois, Urbana, Illinois 61801-3838, United States

ABSTRACT: The second electron transfer from primary ubiquinone Q_A to secondary ubiquinone Q_B in the reaction center (RC) from *Rhodobacter sphaeroides* involves a protonated Q_B^- intermediate state whose low pK_a makes direct observation impossible. Here, we replaced the native ubiquinone with low-potential rhodoquinone at the Q_B binding site of the M265IT mutant RC. Because the in situ midpoint redox potential of Q_A of this mutant was lowered approximately the same extent (≈100 mV) as that of Q_B upon exchange of ubiquinone with low-potential rhodoquinone, the inter-quinone ($Q_A \rightarrow Q_B$) electron transfer became energetically favorable. After subsequent saturating flash excitations, a period of two damped oscillations of the protonated rhodosemiquinone was observed. The $Q_BH^\bullet$ was identified by (1) the characteristic band at 420 nm of the absorption spectrum after the second flash and (2) weaker damping of the oscillation at 420 nm (due to the neutral form) than at 460 nm (attributed to the anionic form). The appearance of the neutral semiquinone was restricted to the acidic pH range, indicating a functional pK_a of <5.5, slightly higher than that of the native ubisemiquinone (pK_a < 4.5) at pH 7. The analysis of the pH and temperature dependencies of the rates of the second electron transfer supports the concept of the pH-dependent pK_a of the semiquinone at the Q_B binding site. The local electrostatic potential is severely modified by the strongly interacting neighboring acidic cluster, and the pK_a of the semiquinone is in the middle of the pH range of the complex titration. The kinetic and thermodynamic data are discussed according to the proton-activated electron transfer mechanism combined with the pH-dependent functional pK_a of the semiquinone at the Q_B site of the RC.

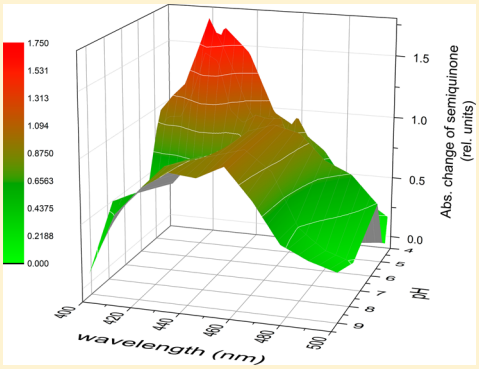

Coupled electron and proton transfers convert energy in many living organisms.[1,2] In the reaction center (RC) protein of photosynthetic bacterium *Rhodobacter sphaeroides*, the light-induced transfer of two electrons to the quinone at the Q_B binding site is accompanied by binding of two protons, resulting in fully reduced hydroquinone QH_2.[3−5] The H^+ ions are taken up from solution by long-range proton transfer (PT) over a distance of ∼15 Å, and a cluster of ionizable residues near the secondary quinone binding site is known to be involved in this delivery pathway. The bacterial RC provides a unique system for understanding the principles of long distance PT. The proton-coupled multielectron reactions, i.e., reactions with intermediate redox states like Q_B (but also others including the water-oxidizing complex of Photosystem II and hydrogenases), need to protect the cofactors from adventitious electron scavenging reactions. A minimum depth of ∼10 Å can be estimated from simple Marcus theory. If the electron transfer (ET) is intermolecular, then the Moser−Dutton rule[6] suggests that the distance should not be greater than 15 Å, which limits the depth at which the charge-accumulating site can be buried. However, if the ET is intramolecular (as for Q_B), the depth is limited by only biosynthetic cost and functional adequacy.[2,7] This necessitates long distance PT if H^+ ions are involved in the reactions. It was shown that the criteria of natural design of long distance PT pathways include the need to provide kinetic competence, high selectivity, and the overarching criterion of evolutionary stability or robustness.[8] A comparison of diverse proton-conducting materials, from gramicidin to cytochrome oxidase, led to the conclusion that rotationally mobile water is a major constituent of proton pathways, for energetic (especially entropic) reasons, and because it provides substantial immunity to mutational catastrophe.[2,8]

On the first ET after the first flash, the RC takes up a nonstoichiometric amount of H^+ ions, reflecting small changes in side chain pK_a values caused by the novel anionic charge of the semiquinone. Depending on the pK_1 of $Q_B^{-\bullet}/Q_BH^\bullet$ and the prevailing pH, the semiquinone itself can also be protonated (Figure 1). After the second flash, protons are delivered directly to the quinone headgroup and the second ET

Received: December 23, 2014
Revised: March 11, 2015
Published: March 11, 2015

DOI: 10.1021/bi501553t
Biochemistry 2015, 54, 2095−2103

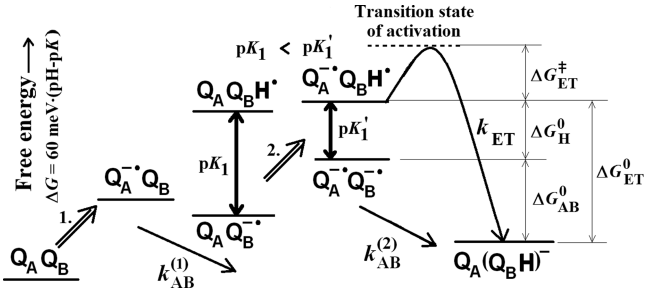

Figure 1. Uptake of the first H^+ ion by $Q_B^{-\bullet}$ in one- and two-electron states of the acceptor quinone complex of the RC after the first and second flashes, respectively. Red arrow 1 represents the light-induced transfer of an electron donor from the primary donor (not shown) to the primary quinone acceptor Q_A followed by the first $Q_A^{-\bullet}Q_B$ to $Q_AQ_B^{-\bullet}$ inter-quinone electron transfer [rate $k_{AB}^{(1)}$]. The generated state is mixed depending upon the proton uptake of $Q_B^{-\bullet}$ determined by the prevailing pH and pK_1 of $Q_B^{-\bullet}$. The second red arrow represents the second light-induced reduction of Q_A followed by the second inter-quinone ET (rate k_{ET}). The second electron transfer occurs from the protonated $Q_BH^\bullet$ semiquinone state whose equilibrium population is determined by pK_1' and the ambient pH. The observed rate of the second ET, $k_{AB}^{(2)}$, is given by eq 1. The free energy levels of the states involved in the proton-coupled ET are indicated for the wild-type RC.

is fully proton-coupled. The analysis of the free energy and pH dependencies of the rate has revealed that the reaction mechanism proceeds via rapid preprotonation of the semiquinone in the two-electron state of the acceptor quinone complex ($Q_A^{-\bullet}Q_B^{-\bullet} \leftrightarrow Q_A^{-\bullet}Q_BH^\bullet$) followed by rate-limiting electron transfer ($Q_A^{-\bullet}Q_BH^\bullet \rightarrow Q_AQ_BH^{-\bullet}$).[9] It is now understood to comprise a rate-limiting ET that is rate-modulated by pH because the protonated semiquinone, $Q_BH^\bullet$, is the actual electron acceptor species. The observed rate is

$$k_{AB}^{(2)} = k_{ET} f(Q_BH^\bullet) \quad (1)$$

where $f(Q_BH^\bullet)$ denotes the population of $Q_BH^\bullet$ and k_{ET} is the (maximal) rate of the forward electron transfer in the quinone complex. For a simple titration

$$k_{AB}^{(2)} = k_{ET} \frac{1}{1 + 10^{pH-pK_2}} \quad (2)$$

The PT equilibrium must be established at least 10 times faster than the rate-limiting ET, at all pH values. How fast the ET rate is, and therefore how fast the PT rate must be, depends on the functional pK_1 of the Q_B semiquinone. For the native ubiquinone$_{10}$ in RC of *Rba. sphaeroides*, the pK_1 should be very low as the Q_B^- semiquinone remains fully anionic at least down to pH 4.5, and therefore, the neutral (protonated) semiquinone as the transition intermediate of the second ET cannot be observed.[10,11]

A straightforward suggestion is to replace the ubiquinone at the Q_B site with a different type of quinone that can forward electrons and protons to quinol formation, and its semiquinone form exhibits a pK value higher than that of ubisemiquinone. Rhodoquinone (RQ) seems to fulfill these conditions. It is a required cofactor for anaerobic respiration in *Rhodospirillum rubrum*.[12] RQ is an aminoquinone that is structurally similar to ubiquinone (UQ), a ubiquitous lipid component involved in the aerobic respiratory chain. The only difference between the structures is that RQ has an amino group (NH_2) on the benzoquinone ring in place of a 3-methoxy substituent (OCH_3) in UQ. This difference of the structures causes considerable differences in (i) the redox midpoint potentials (E_m) measured polarographically {at pH 7, −63 mV for RQ and +43 mV for UQ (ubiquinone-10) in a mixture of ethanol and water [4:1 (v/v)] and −30 mV (RQ) and +50 mV (UQ) bound to chromatophores of *Rh. rubrum*}[13] and (ii) the pK of protonation of the semiquinones. The plots of the polarographic E_m versus pH curves can be used to estimate the numbers of electrons (e^-) and H^+ ions in the electrode reactions, but the plots fail to determine the increase in the pK of $RQ^{-\bullet}/RQH^\bullet$ relative to that of $UQ^{-\bullet}/UQH^\bullet$.[14] The shift is probably due to the higher level of electron donation of the amino substituent in RQ than the methoxy group in UQ to the quinone ring. The pK of rhodosemiquinone was estimated to be 7.3 at the Q_B site of the RC.[15] These results, however, must be regarded as very tentative because of the absence of more fundamental electrochemical information.[16]

The reduction of the low-potential rhodoquinone at the Q_B binding site requires the use of low-potential analogues of Q_A[15] or direct ET to Q_B along the inactive B branch.[17] Both methods have difficulties. Binding of different (non-native) quinones in the Q_A and Q_B sites calls for great challenge in the RC of *Rba. sphaeroides*. The incomplete binding of the quinones results in restricted inter-quinone ET with a mixture of Q_A^- and Q_B^- states after the first saturating flash. The observation of B branch ET to Q_B needs heavily modified RC with a total of five mutations, and even in that case, the quantum yield of Q_B reduction is very low (~5%). Because the many modified residues are not located in the region around Q_B, the integrity of the Q_B environment is supposed to be preserved.[18]

In this work, we used a different procedure for reducing rhodoquinone in the Q_B site. The Q_A binding site remained occupied by the native ubiquinone, but its redox midpoint potential was lowered by 100−120 mV upon mutation of M265 isoleucine to the smaller, polar residue of threonine in the Q_A binding pocket.[19] The H-bond structure and the extensive decrease in the redox midpoint potential of Q_A were studied earlier by delayed fluorescence of the bacteriochlorophyll dimer,[20,21] Fourier transform infrared,[22] and magnetic resonance[23] spectroscopy and quantum mechanical calculations of the ^{13}C couplings of the 2-methoxy dihedral angle.[24,25] The large decrease in the redox potential of Q_A is attributed to hydrogen bonding of the OH to the peptide C=O of ThrM261, which causes a displacement of the backbone strand that bears the hydrogen bond donor (AlaM260) to the C1 carbonyl of Q_A, lengthening the hydrogen bond to the semiquinone state, Q_A^-, and thereby destabilizing it. This greatly increases ΔE_m, the driving force for ET. If we combine the two low-potential quinones at Q_A (M265IT mutant) and Q_B (RQ substitution) sites, the driving force will remain sufficiently large to obtain efficient inter-quinone ET. We will have a chance to recognize the protonation of the semiquinone either from the typical light-induced optical absorption spectrum between 400 and 500 nm[26] or from comparison of the damping of the semiquinone oscillation[27] detected at wavelengths characteristic of the neutral and anionic forms of the semiquinone at the Q_B site of the RC.

MATERIALS AND METHODS

Chemicals and Reaction Centers. UQ_{10} (ubiquinone$_{10}$, 2,3-dimethoxy-5-methyl-6-decaisoprenyl-1,4-benzoquinone) was purchased from Sigma. RQ (rhodoquinone; 2-amino-3-methoxy-6-methyl-5-decaisoprenyl-1,4-benzoquinone) was ob-

DOI: 10.1021/bi501553t
Biochemistry 2015, 54, 2095−2103

tained from *Rh. rubrum* grown photosynthetically under anaerobic conditions.[28] Separation of RQ from the quinone extractions was performed using preparative TLC plates.[29,30] The concentration of RQ in ethanol was determined from optical absorption coefficient of 1 mM^{-1} cm^{-1} at 500 nm.[31] Ferrocene (Eastman Kodak) and terbutryne (Chem. Service) used to reduce the oxidized dimer (P) and to block the inter-quinone electron transfer, respectively, were solubilized in ethanol. The buffer mix contained the following buffers (1−1 mM): 2-(*N*-morpholino)ethanesulfonic acid (MES, Sigma), succinate, or citric acid (Calbiochem) between pH 4.5 and 6.5; 1,3-bis[tris(hydroxymethyl)methylamino]propane (Bis-Tris propane, Sigma) between pH 6.3 and 9.5; Tris-HCl (Sigma) between pH 7.5 and 9.0; and 3-(cyclohexylamino)-propanesulfonic acid (CAPS, Calbiochem) above pH 9.5.

The details of the molecular biological techniques in generating the M265IT mutant from strain *Rba. sphaeroides*, the cultivation, and the preparation of RC protein have been described previously.[19] The UQ at the Q_B site was removed as described previously[32] and reconstituted by addition of RQ in large (>10) excess over RC. The occupancy of the Q_B site was >70% as determined from the ratio of the amplitudes of the slow and fast phases of the charge recombination measured at 865 nm.

Electron Transfer Measurements. The kinetics of flash-induced ET was measured by absorption changes using a single-beam spectrophotometer of local design.[33] The rates of charge recombination ($P^+Q_B^-$ → PQ_B) were obtained by monitoring the recovery of the dimer (P) absorbance at 430 nm (or 865 nm), following a saturating exciting flash. Electron transfer rate $k_{AB}^{(1)}$ ($Q_A^{-\bullet}Q_B$ → $Q_AQ_B^{-\bullet}$) was measured by tracking the absorption change at 398 nm following a saturating flash. The rate constants of the second ET to $Q_B^{-\bullet}$ were determined by monitoring the decay of semiquinone absorbances ($Q_A^{-\bullet}$ and $Q_B^{-\bullet}$) at a wavelength of 450 nm following a second saturating flash in a RC solution containing the exogenous reductant, ferrocene, which reduced the oxidized dimer P^+ within 1−5 ms.[11,34]

RESULTS

Rate and Temperature Dependence of $P^+Q_A^-$ Charge Recombination in the M265IT Mutant RC. The kinetics of P^+ dark decay following a flash was measured at 430 nm in the M265IT RC with native UQ at the Q_A binding site and empty Q_B binding site (Figure 2). The observed k_{AP} rates were 2−3 times faster than those for the wild-type RC[19] and showed temperature dependence. The Arrhenius plot of the temperature dependence of k_{AP} is presented in the inset of Figure 2: $\ln(k_{AP})$ follows a straight line revealing activation energy. The increased k_{AP} rates together with the temperature dependence suggest a thermally activated process of charge recombination and indicate that the free energy of the $P^+Q_A^-$ state in the M265IT mutant has been increased so that this state decays no longer directly to the PQ_A ground state by a tunneling effect. When the redox potential of Q_A is sufficiently low, a different pathway opens in which the electron is thermally excited to the relaxed state (M) of P^+I^- (I is bacteriopheophytin) with subsequent rapid decay from M to PQ_A.[35−37] The observed rate of $P^+Q_A^-$ recombination becomes

$$k_{AP} = k_d \times \exp\left(\frac{-\Delta G_{AM}^{\circ}}{RT}\right) \quad (3)$$

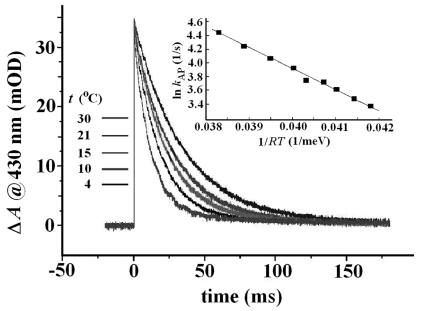

Figure 2. Temperature dependence of the kinetics of the $P^+Q_A^-$ → PQ_A charge recombination measured by a flash-induced absorption change at 430 nm of the M265IT mutant RC of *Rba. sphaeroides*. The increasing rate constant k_{AP} of charge recombination with an increase in temperature is an indication of low-potential quinone at the Q_A binding site (inset). The shift in the free energy level of $P^+Q_A^-$ in the M265IT mutant relative to that of the wild type amounts to a ΔG_{QA}° of 107 meV (see the text). Conditions: 1.1 μM RC (Q_B-depleted), 0.03% LDAO, 1 mM MOPS buffer, and 2.5 mM KCl (pH 7).

where R is the universal gas constant, T is the temperature, and ΔG_{AM}° is the free energy gap between M and $P^+Q_A^-$ that is controlled by the equilibrium redox potential of Q_A/Q_A^-. The pre-exponential factor ($k_d = 2 \times 10^7$ s^{-1}) is the effective rate of recombination of P^+I^- to the ground state and is independent of the nature of the M265IT mutation.[35,36]

According to eq 3, the thermodynamic parameters of the recombination of the M265IT mutant can be derived from the slope ($-\Delta H$, change in enthalpy of the back reaction) and interception [$\ln(k_d) + \Delta S/T$, where ΔS is the change in entropy of the recombination] of the straight line in the Arrhenius plot. As we obtained a ΔH of 305 ± 10 meV and a $T\Delta S$ of −18 ± 1 meV for the enthalpic and entropic components of the free energy gap, respectively, $\Delta G_{AM}^{\circ} = \Delta H - T\Delta S = 323 \pm 11$ meV can be derived. The free energy gap (ΔG_{AM}°) between M and $P^+Q_A^-$ states in wild-type *Rba. sphaeroides* was found to be 430 meV.[35,37] Therefore, the free energy level of $P^+Q_A^-$ in the M265IT mutant is found to be increased by 430 meV − 323 meV = 107 meV (±11 meV); i.e., the shift of the midpoint redox potential of Q_A in M265IT relative to that of WT amounts to −110 mV at pH 7. This value is in excellent agreement with that obtained by delayed fluorescence measurements of the dimer.[20]

Q_B Site of M265IT Occupied by RQ. Upon addition of RQ to the Q_B-depleted RC, a slow phase with an ~(500 ms)$^{-1}$ rate constant appears in the charge recombination kinetics that disappears in the presence of the potent inhibitor terbutryne (data not shown). Subsequent saturating flashes evoke binary oscillation of the semiquinone in the presence of an external electron donor to the oxidized dimer, P^+ characteristic of the two-electron gate function of Q_B[10,38] (Figure 3). If UQ occupies the Q_B binding site of the M265IT mutant RC, then the oscillations in Q_B^- semiquinone formation are at least as strong as in wild-type RCs, consistent with a large value of electron equilibrium constant and effective transfer of the second electron.[19] If, however, RQ replaces UQ at the Q_B binding site, the magnitude of the semiquinone oscillation is significantly affected and the damping will be larger. The damping of the oscillation of the rhodosemiquinone upon subsequent saturating flashes is determined by (i) the occupancy of the Q_B site ($1 - \delta$) and (ii) the one-electron equilibrium partition coefficient [$\alpha = [Q_A^-Q_B]/([Q_A^-Q_B] +$

DOI: 10.1021/bi501553t
Biochemistry 2015, 54, 2095−2103

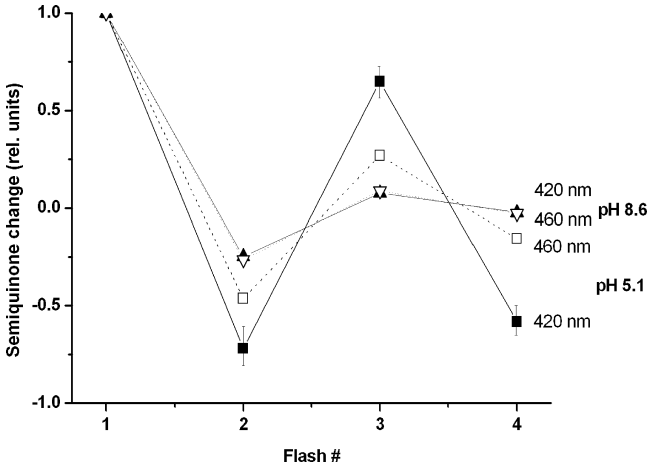

Figure 3. Changes of rhodosemiquinone at the Q_B site of the M265IT mutant RC upon subsequent saturating flashes measured at two wavelengths, 420 nm (characteristic of protonated RQ, $RQ_BH^{\bullet}$) and 460 nm (characteristic of the anionic form of RQ, $RQ_B^{-\bullet}$), and two pH values (5.1 and 8.6). The magnitudes are normalized to the change evoked by the first flash. The lines were fit by $\delta = 0.2$ and $\alpha = 0.09$ (pH 5.1 and 420 nm), 0.42 (pH 5.1 and 460 nm), 0.69 (pH 8.6 and 420 nm), and 0.67 (pH 8.6 and 460 nm) (see eq 4). Conditions: 1.1 μM RC, 100 μM RQ, 0.02% LDAO, 60 μM ferrocene, 5 mM buffer mix, and a flash repetition rate of 5 Hz.

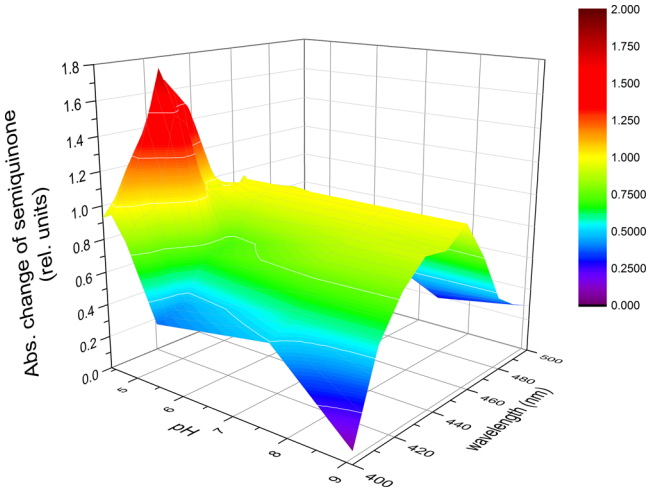

Figure 4. Quasi three-dimensional representation of the optical absorption spectra of rhodosemiquinone at the secondary quinone binding site (Q_B) of the M265IT mutant RC measured after a saturating flash in the presence of an electron donor to the oxidized dimer P^+ at several pH values. The 420 nm band of the spectra at low pH resembles the protonated spectrum of semiquinone in solution.[26] The spectra are normalized to the absorption at 450 nm.

$[Q_AQ_B^-])]$ in the acceptor quinone system.[27] The measured semiquinone absorption contains contributions from both Q_A^- and Q_B^- (protonated or deprotonated) and is given after the nth (>0) saturating flash by

$$\Delta A_n = (1-\delta)\frac{1-(-1)^n(1-\alpha)^n}{2-\alpha} + \delta \qquad (4)$$

which is normalized to the absorption change after the first flash, ΔA_1. Figure 3 demonstrates the change in the semiquinone content after the nth flash: $\Delta Q^-_n = \Delta A_n - \Delta A_{n-1}$, i.e., the difference between two sequential flashes. By fitting the measured data to the model, we get $\delta = 0.2$ (the occupancy of the Q_B site by RQ is 80% in this experiment) and pH- and wavelength-dependent partition coefficients. At low pH, the damping is small, indicating effective electron transfer to Q_B. The oscillation at 420 nm (characteristic of protonated RQ, $RQ_BH^{\bullet}$) is larger than at 460 nm (typical of the anionic form of RQ, $RQ_B^{-\bullet}$) expressed by the smaller α at 420 nm than at 460 nm (0.09 and 0.42, respectively). At low pH (<pK_1), the protonated form of Q_B^- involves a free energy level lower than that of the anionic form (Figure 1). Therefore, because of the contribution of $RQ_BH^{\bullet}$, a smaller partition coefficient (higher one-electron equilibrium constant) was obtained. In crude terms, the protonation stabilizes the semiquinone state. At high pH (8.6), the oscillation is strongly damped and no distinctions can be made according to wavelengths: $\alpha = 0.69$ and 0.67 at 420 and 460 nm, respectively. The rhodosemiquinone is not protonated at all in this pH range.

This indirect statement can be confirmed by direct measurement of the second flash-induced absorption spectra of rhodosemiquinone in the 400−500 nm spectral range at different pH values (Figure 4). The generated spectral pofile is attributed mainly to the (anionic or ionic forms) of the Q_B semiquinone[26] as the spectral contribution of the oxidized external donor (ferrocinium) in this region and the accumulation of the $Q_A^{-\bullet}$ species are negligible. Similar spectra were obtained when the semiquinone appeared (after an odd number of flashes) or disappeared (after an even number of flashes), indicating that the contribution of RQ_B^- played the determining role. The spectra consisted of components from protonated RQ (characteristic band around 420 nm that appeared below pH 5) and deprotonated (anionic) RQ (characteristic band at 450 nm that dominates above pH 5). Although the appearance and disappearance of the band at 420 nm can be well recognized at low and neutral pH ranges, respectively, it is hard to predict a characteristic pK value for protonation of RQ_B^- as its band did not attain obviously its maximum at the lowest pH value (pH 4.3) used in these measurements. We predict a pK of ≤5 that is significantly smaller than 7.3 obtained after a simple (not extended) Henderson−Hasselbalch titration curve in ref 15.

Electron Transfer Rates. The exchange of UQ for RQ at the Q_B site of M265IT has a much larger effect on the energetics of the quinone acceptor system (manifested by variations of the $P^+Q_B^- \rightarrow PQ_B$ charge recombination or semiquinone oscillation) than on the kinetics of the first ($Q_A^-Q_B \rightarrow Q_AQ_B^-$) and second ($Q_A^-Q_B^- \rightarrow Q_AQ_BH$) electron transfers. The rates of the $k_{AB}^{(1)}$ reaction were the same with UQ as with RQ in the Q_B site (data not shown). Because the rate of the first electron transfer is under the control of conformational gating of the Q_B site,[39] the result indicates that substitution of RQ does not affect the dynamics of Q_B motion. The rates of the second ET with UQ or RQ at the Q_B site show similar and noninteger pH dependence below pH 8 (Figure 5). They demonstrate a highly moderate pH dependence at low pH (~0.1 decade/pH unit) but decrease at high pH by a factor of 10 per pH unit. For RQ, the rates are slightly smaller and the crossing point of the lines that approximate the low- and high-pH behavior has a pH value higher than those for UQ.

The rate of the second electron transfer is sensitive to the temperature: it increases upon elevation of the temperature in the physiological range. Figure 6 demonstrates this dependence for UQ and RQ at the Q_B site at different pH values in Arrhenius-type representation where the logarithm of the rate is

DOI: 10.1021/bi501553t
Biochemistry 2015, 54, 2095−2103

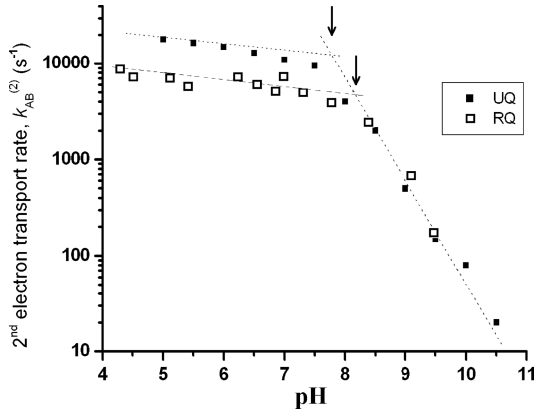

Figure 5. pH dependence of the rate of the second electron transfer in the M265IT mutant RC whose Q_B is occupied by either native UQ (■) or RQ (□). The rate was measured from the decay of semiquinone absorbance at 450 nm after the second flash. The lines represent the approximate weak pH dependence below pH 8 (~0.1 decade per pH unit) and the theoretical 1 decade/pH unit drop above pH 8. Note the shift of the crossing point of the straight lines upon UQ–RQ exchange at Q_B. Conditions: 2 μM RC in 2.5 mM KCl, 1 mM buffer mix, 0.02% LDAO, 40 μM UQ_{10} or 100 μM RQ_{10}, and 2–200 μM ferrocene (or its derivatives), depending on the rate (or pH).

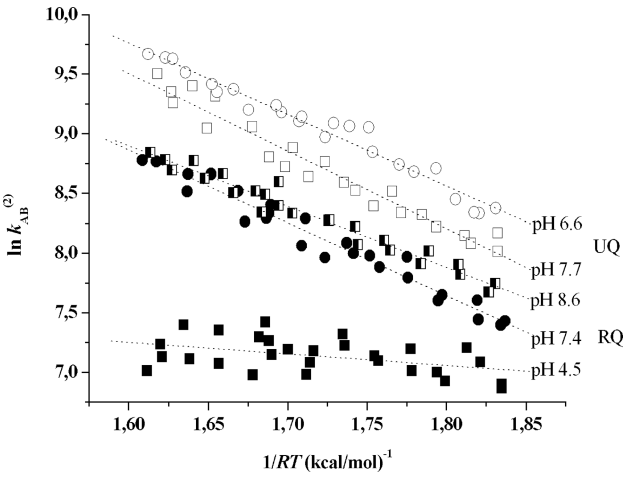

Figure 6. Temperature dependence of the rate of the second electron transfer at the physiological temperature range in the M265IT mutant RC with UQ (empty symbols) and RQ (filled symbols) at the Q_B binding site at several pH values. Conditions as in Figure 5. The fitted parameters of the straight lines (slope and intercept) are used to determine the thermodynamic parameter of activation of the second ET (see Table 1).

plotted as a function of the reciprocal of the temperature. As the measured data fit to straight lines, one can formally introduce observed activation parameters for the temperature dependence of the second ET:

$$k_{AB}^{(2)} = k_{max} \times \exp\left(-\frac{\Delta G_{obs}^{\ddagger}}{RT}\right) \quad (5)$$

where $k_{max} \approx 3.5 \times 10^9$ s^{-1} obtained from the exchange coupling between Q_A^- and Q_B^- in EPR studies,[40] R and T are the universal gas constant and the absolute temperature, respectively, and $\Delta G_{obs}^{\ddagger}$ is the observed free activation energy that can be decomposed into the enthalpy change of activation, $\Delta H_{obs}^{\ddagger}$ and entropic change of activation, $T\Delta S_{obs}^{\ddagger}$ ($\Delta G_{obs}^{\ddagger} = \Delta H_{obs}^{\ddagger} - T\Delta S_{obs}^{\ddagger}$). They can be derived from the slope (Slope) and interception (Int) of the straight line $\Delta H_{obs}^{\ddagger} = -$slope and $T\Delta S_{obs}^{\ddagger} = RT[\text{Int} - \ln(k_{max})]$. Their values are listed in Table 1. As one can see, neither the rates nor the activation parameters are very much different if UQ is replaced by RQ at the Q_B binding site of the M265IT mutant RC.

■ DISCUSSION

The results confirmed the incorporation of RQ into the Q_B site (~80%) and the reconstitution of the Q_B activity. It was demonstrated that the drop of the midpoint redox potential of Q_A in the M265IT mutant was large enough to compensate largely for a similar shift in the midpoint redox potential of Q_B when UQ was replaced by the low-potential RQ. Although the driving force and the electron equilibrium constants in the quinone complex became smaller, effective inter-quinone ET and turnover of the RC could be measured. The discussion will focus on the pH-dependent pK values of the Q_B^- semiquinones and the decomposition of the observed activation free energy of the second ET into contributions of both proton and electron transfer steps.

pK Values of Semiquinone at the Q_B Site. The pK of the ubisemiquinone has been estimated at $pK_1 \approx 3.8$ for the $(Q_A)Q_B^-/Q_BH$ one-electron equilibrium and $pK_1' \approx 4.5$ for the $(Q_A^-)Q_B^-/Q_BH$ two-electron equilibrium valid at pH 7.5.[4,41] These are mildly suppressed from the value in aqueous solution ($pK_a \approx 4.9$), but more importantly, the RC value appears to be pH-dependent because of the changing charge distribution, and possibly sensitive to the nature of the environment, i.e., detergent versus native membrane. Several acidic groups with Q_B^- constitute a cluster of strongly interacting components resulting in a remarkable and unexpected pH dependence of flash-induced proton uptake.[42] The protonation of the semiquinone does not follow a simple titration curve, and to preserve the formalism, pH-dependent pK values should be introduced.[41] The weak pH dependence of the rate of the second ET up to pH 8 suggests that the pK of the semiquinone is not constant but is continuously modulated by interactions with a changing electrostatic environment. Recently, a molecular probe (stigmatellin) was introduced to measure the electrostatic potential at the Q_B site.[43] The apparent pK of the semiquinone at a definite pH depends on minor changes in the intrinsic pK_a values of Q_B^- and the amino acids involved, and on their strengths of interaction. By measuring the decrease of the rate constant of the second ET in several mutants, we observed a considerable decrease in the operational pK of Q_B^-/Q_BH with a change of a single amino acid at key positions: the estimated pK of 4.5 (native) dropped to 3.9 (L210DN), 3.7 (M17DN), and 3.1 (H173EQ) at pH 7.[11] The results may simply suggest that the point at which pK approaches and exceeds the ambient pH (thereby allowing significant levels of $Q_BH^•$) will depend on interaction with components of the acidic cluster.

While the values of the pK of ubisemiquinone fall in the lower part, the pK for rhodosemiquinone lies at the upper limit of the range of those of carboxylates (4–5), where the protein electrostatics are most complex. A similar type of interaction as discussed above for UQ may be responsible for the increase in the operational pK of rhodosemiquinone that was large enough to be able to measure the protonated rhodosemiquinone below pH 5.5. The estimated pK, however, was much smaller in our study than that reported previously.[15] The lower pK value was supported by recent low-temperature electron paramagnetic

DOI: 10.1021/bi501553t
Biochemistry 2015, 54, 2095–2103

Table 1. Standard (°) and Activation (‡) Free Energy (ΔG), Enthalpy (ΔH), and Entropic Energy ($T\Delta S$) Changes of the Second Electron Transfer in the M265IT RC with either UQ or RQ at the Q_B Binding Site[a]

RC	Q_B site	pH	$\Delta H^{\ddagger}_{obs}$ (kcal/mol)	$T\Delta S^{\ddagger}_{obs}$ (kcal/mol)	$\Delta G^{\ddagger}_{obs}$ (kcal/mol)	ΔG°_{H} (kcal/mol)	pK_2	ΔG°_{ET} (kcal/mol)	$\Delta G^{\ddagger}_{ET}$ (kcal/mol)	k_{ET} (μs^{-1})
M265IT	UQ	6.6	6.0	−1.5	7.5	3.3	3.8	−7.0	3.9	4.4
	UQ	7.7	6.1	−2.0	8.1	4.2	4.3	−7.9	3.6	7.6
	RQ	4.5	6.5	−1.2	7.7	2.3	2.6	−3.6	5.2	0.4
	RQ	7.4	5.1	−2.9	8.0	2.7	5.2	−4.1	5.0	0.6
	RQ	8.6	1.0	−7.6	8.6	3.9	5.6	−5.2	4.6	1.4
WT	UQ	7.8	4.2	−4.8	9.0	4.8	4.3	−6.2	4.2	2.6

[a]The observed activation parameters were obtained from the temperature dependence of $k^{(2)}_{AB}$ and the free energies ΔG°_{H}, ΔG°_{ET}, and $\Delta G^{\ddagger}_{ET}$ were calculated from eqs 10, 9, and 8, respectively. The values of pK_2 and k_{ET} were derived from the equations $\Delta G^{\circ}_{H} = 2.3RT(pH - pK_2)$ and $k_{ET} = k_{max} \times \exp(-\Delta G^{\ddagger}_{ET}/RT)$, respectively. For the maximal electron transfer rate, $k_{max} = 3.5 \times 10^9\ s^{-1}$;[40] for the reorganization energy, $\lambda = 1.2$ eV,[15] and for the free energy gap between the quinones in two-electron states, $\Delta G^{\circ}_{AB} = -60$ meV (UQ in WT and RQ in M265IT) and $\Delta G^{\circ}_{AB} = -160$ meV (UQ in M265IT).[19,20]

resonance (EPR) and electron nuclear double-resonance (ENDOR) investigations in which no changes of the spectra were found with a decrease in pH from the alkaline to the acidic range as low as pH 4.5.[17]

The protonated ubisemiquinone in isolated RC (UQ^{-}_{B}) has a very low pK value (~4.0), similar (4.1) to the pK_a of the protonated 1,4-semiquinone radical.[44,45] Substituents on the quinone ring can influence the electron density on the ring and thus modify both the redox midpoint potential and pK values.[46] The hydroxy groups increase slightly the pK. Because of the properties of electron donation of methyl groups into the ring, the methyl groups increase the pK by ~0.25 pH unit/group. The effect of methoxy groups is very similar to that of the methyl groups. The substitution of amino groups in 9,10-anthraquinone (AQ) gives a hint of the magnitude of the pK shift in RQ relative to UQ. The pK_1 of AQ was found to be 5.3[46,47] that increased by $\Delta pK = 0.5$ to pK_1 = 5.8 in 1-amino-AQ.[48]

It is well-established that spatial orientations and restrictions of the substituents can seriously modify the electron donating capacity.[24,25] While the 2-methoxy group of UQ is free for conformational change and takes an out-of-plane conformation in the Q_B binding pocket, the 3-methoxy group is unable to conduct a similar conformational change, probably because of steric restriction *in situ*. In RQ, this position is substituted with an amino group; therefore, no significant contribution can be expected from conformation-related pK changes. The observed and predicted changes in pK published in the literature for different substituents support our results of a moderate (1−1.5) increase in the pK of rhodosemiquinone with respect to ubisemiquinone.

In chromatophores, the protonation of the stable Q_B ubisemiquinone ($Q_AQ_BH^{\bullet}$) was readily observable, with a functional pK of 6.[49] This also suggests slight changes in the interactions of the RC embedded in chromatophores relative to isolated RC. In addition to the functional pK for Q_B^{-}, other differences may exist between isolated RCs and chromatophores. The midpoint redox potential of the primary quinone, $E_m(Q_A^{-}/Q_A)$, is strongly pH-dependent in chromatophores[50] but not in isolated RCs.[51,52] However, determinations of the free energy gap between P* and $P^{+}Q_A^{-}$ in chromatophores reveal a pH dependence identical to that seen in isolated RCs and cast serious doubt on the potentiometric determinations of $E_m(Q_A^{-}/Q_A)$ probably because of poor mediation of the Q_A binding site of the protein.[53] It was suggested that Q_A may actually be titrated through the Q_B site, reflecting titration of the quinone pool or perhaps a redox mediator in the Q_B site. Nevertheless, this remained an open question whose answer is critical to our understanding of the acceptor quinones.

The semiquinone has two different pK values in one-electron (pK_1) and two-electron (pK_1') states of the quinone acceptor complex (Figure 1). We were able to determine the pK_1 from the oscillation of the flash-induced absorption changes of the stable semiquinone, when Q_A was oxidized. The determination of pK_1' of the transient semiquinone important in the second ET is not straightforward, but a realistic estimate can be offered. The difference between pK_1 and pK_1' is due to the extra (electrostatic) interaction of Q_A^{-} with Q_B^{-} that can be deduced from equilibrium and kinetic electron transfer and proton uptake measurements and electrostatic calculations. The long-range interactions between the two quinone sites prepare the Q_B site for the subsequent electron transfer from Q_A.[54] The electrostatic influence of Q_A^{-} on the apparent pK_a of the acidic cluster that controls the pH dependence of the electron equilibrium in the quinone complex causes a difference of 0.5−1 unit between pK values in states Q_AQ_B and $Q_A^{-}Q_B$.[41] This result is consistent with the conclusions drawn from the pH dependence of the H^{+}/Q_A^{-} and H^{+}/Q_B^{-} stoichiometries.[33,55] Light activation causes proton uptake as the acid cluster reprotonates in accordance with the pK shifts induced by the semiquinone anions. The pH dependence of the H^{+} uptake stoichiometries, H^{+}/Q_A^{-} and H^{+}/Q_B^{-}, can be deconvoluted into discrete contributions. Q_A^{-} causes pK shifts of 0.7−0.8 pH unit estimated for the pK_1' of the Q_B semiquinone in the two-electron state, $Q_A^{-}Q_B^{-}$, and for the first pK of the quinol, QH^{-}, in the three-electron state, $Q_A^{-}Q_BH^{-}$.[15,56] The 0.7−0.8 unit upshift in the pK of the ubiquinone in the $Q_A^{-}Q_B^{-}$ state was similar to that inferred for the rhodoquinone occupant.[15] In this work, the protonation of the rhodosemiquinone was observed in the one-electron state ($Q_AQ_B^{-} \leftrightarrow Q_AQ_BH$) with a p$K_1$ of 7.3. On the second electron transfer, $k^{(2)}_{AB}$ displayed a well-behaved pH dependence (see eq 2 with a pH-independent pK): it was constant below pH 7 and decelerated 10-fold per pH unit above a pK of 8.0 in the $Q_A^{-}Q_B^{-}$ state. In contrast, our kinetic and thermodynamic data were consistent with the significantly smaller and pH-dependent functional pK_1 of the rhodosemiquinone.

Activation Analysis of the Second ET. The fast proton pre-equilibrium is followed by a rate-limiting ET. The states involved in the $k^{(2)}_{AB}$ reaction are shown in Figure 1. The observed activation parameters are characteristic to both the proton equilibrium and the subsequent electron transfer step. On one hand, the rate of the second ET increases with a decrease in the activation barrier, $\Delta G^{\ddagger}_{ET}$, and on the other hand

DOI: 10.1021/bi501553t
Biochemistry 2015, 54, 2095−2103

decreases due to the increase in the free energy to protonate the semiquinone [$\Delta G^{\circ}_{H} = 2.3RT(pH - pK_2)$] that results in a smaller population of the $Q_B^{-\bullet}$ state. The connected proton and electron transfer steps give the complex behavior of the apparent activation. Whatever rate model is used for the ET, the proton pre-equilibrium (acid association) parameters (ΔG°_{H}, etc.) combine with those of the true activation step ($\Delta G^{\ddagger}_{ET}$, etc.) to give the observed activation energies ($\Delta G^{\ddagger}_{obs}$, etc.) that will not be, however, simply the sum of the components.

The rate-limiting step is a nonadiabatic ET, and the Marcus formalism should be used.[57]

$$k^{(2)}_{AB} = \frac{k_{max} \times \exp\left(-\frac{\Delta G^{\ddagger}_{ET}}{RT}\right)}{1 + \exp\left(\frac{\Delta G^{\circ}_{H}}{RT}\right)} \quad (6)$$

If eqs 5 and 6 are compared, then

$$\Delta G^{\ddagger}_{obs} = \Delta G^{\ddagger}_{ET} + RT \times \ln\left[1 + \exp\left(\frac{\Delta G^{\circ}_{H}}{RT}\right)\right] \quad (7)$$

Here, the activation free energy of ET, $\Delta G^{\ddagger}_{ET}$, can be expressed from the free energy of the ET (defined as the free energy of the final minus the initial state), ΔG°_{ET}, and the reorganization energy, λ:

$$\Delta G^{\ddagger}_{ET} = \frac{(\Delta G^{\circ}_{ET} + \lambda)^2}{4\lambda} \quad (8)$$

The standard free energy levels follow a simple summation rule. The free energy for electron transfer, ΔG°_{ET}, is the difference in the free energy between initial and final states, ΔG°_{AB}, and the free energy to protonate $Q_B^{-\bullet}$, ΔG°_{H}:

$$\Delta G^{\circ}_{ET} = \Delta G^{\circ}_{AB} - \Delta G^{\circ}_{H} \quad (9)$$

.

Inserting eq 9 into eq 8 and inserting eq 8 into eq 7, we obtain

$$\Delta G^{\ddagger}_{obs} = \frac{(\Delta G^{\circ}_{AB} - \Delta G^{\circ}_{H} + \lambda)^2}{4\lambda} + RT \times \ln\left[1 + \exp\left(\frac{\Delta G^{\circ}_{H}}{RT}\right)\right] \quad (10)$$

ΔG°_{H} and pK_2 at a definite pH can be obtained by solution of eq 10 with λ = 1.2 eV (=27.7 kcal/mol)[15] and ΔG°_{AB} = −160 meV for UQ[19,20] and ΔG°_{AB} = −60 meV for RQ at the Q_B site. Although the latter values refer to the differences in free energy between the semiquinones in one-electron states, similar values can be taken for the two-electron states. In the WT RC, a very small (β < 0.05) partition coefficient was found for the two-electron equilibrium in the acceptor quinone system at pH <8.[58] The measured and calculated values are listed in Table 1. The functional (pH-dependent) pK_1' values are somewhat higher for RQ than for UQ. Although the increase is not as large as reported previously,[15] a fraction of protonated RQ could be detected in our experiments in the low-pH range (see Figure 4). This observation is in good agreement with conclusions of recent EPR and ENDOR studies.[17]

The $T\Delta S^{\ddagger}_{obs}$ entropy change is small and negative. The negative value makes sense as an activation parameter. By our estimates, the entropic component from the electron transfer, $T\Delta S^{\ddagger}_{ET}$, is quite small and pH-independent. Most of the observed activation entropy is due to the protonation equilibrium, i.e., entropy of mixing. Accordingly, it should have an increasingly negative entropy contribution with pH. Indeed, the entropy of activation decreases (becomes more negative) because H^+ ions are being brought from an increasingly dilute solution as the pH is increased.

CONCLUSIONS

With a decrease in the potential of the UQ at the Q_A site in the M265IT mutant, the activity of the Q_B site occupied by the low-potential RQ can be reconstituted. The second electron transfer reaction followed the mechanism of proton-activated electron transfer. The flash-induced rhodosemiquinone showed partly neutral (protonated) character below pH 5 and was completely anionic above pH 5.5. Kinetic and thermodynamic assays of the second ET supported the low value of the functional pK of RQ at the Q_B site that was slightly higher than that of the native ubiquinone. The pK is pH-dependent because of the pH-dependent local potential whose main contributor is the cluster of acidic residues around Q_B. The complex deprotonation of the cluster makes the positive local potential at low pH gradually more and more negative at high pH. The pH dependence of the pK is responsible for the fact that the second ET rate has a noninteger pH dependence below pH 8.

AUTHOR INFORMATION

Corresponding Author

*Department of Medical Physics, University of Szeged, Rerrich Béla tér 1., Szeged, Hungary H-6720. Phone: 36-62-544-120. Fax: 36-62-544-121. E-mail: pmaroti@sol.cc.u-szeged.hu.

Funding

This work was supported by TÁMOP 4.2.2.A-11/1KONV-2012-0060, TÁMOP 4.2.2.B, COST CM1306, and OTKA K116834.

Notes

The authors declare no competing financial interest.

ACKNOWLEDGMENTS

Thanks to Dr. E. Takahashi (University of Illinois) for the M265IT mutant and to G. Sipka (University of Szeged) for the three-dimensional representation of Figure 4.

DEDICATION

†Deceased July 10, 2014. This work is dedicated to his memory.

ABBREVIATIONS

ET, electron transfer; P, bacteriochlorophyll dimer; QA and QB, primary and secondary quinone acceptors, respectively; UQ10, ubiquinone; RC, (bacterial) reaction center; RQ, rhodoquinone.

REFERENCES

(1) Cramer, W. A., and Knaff, D. B. (1990) *Energy Transduction in Biological Membranes: A Textbook of Bioenergetics*, Springer-Verlag, New York.

(2) Wraight, C. A. (2006) Chance and design: Proton transfer in water, channels and bioenergetic proteins. *Biochim. Biophys. Acta 1757*, 886−912.

DOI: 10.1021/bi501553t
Biochemistry 2015, 54, 2095−2103

(3) Okamura, M. Y., Paddock, M. L., Graige, M. S., and Feher, G. (2000) Proton and electron transfer in bacterial reaction centers. *Biochim. Biophys. Acta 1458*, 148−163.
(4) Zhu, Z., and Gunner, M. R. (2005) Energetics of quinone-dependent electron and proton transfers in *Rhodobacter sphaeroides* photosynthetic reaction centers. *Biochemistry 44*, 82−96.
(5) Wraight, C. A., and Gunner, M. R. (2009) The Acceptor Quinones of Purple Photosynthetic Bacteria- Structure and Spectroscopy. In *Advances in Photosynthesis and Respiration: The Purple Phototrophic Bacteria* (Hunter, C. N., Daldal, F., Thurnauer, M., and Beatty, J. T., Eds.) pp 379−405, Springer, Dordrecht, The Netherlands.
(6) Moser, C. C., Page, C. C., Cogdell, R. J., Barber, J., Wraight, C. A., and Dutton, P. L. (2003) Length, Time and Energy Scales of Photosystems. *Adv. Protein Chem. 63*, 71−109.
(7) Takahashi, E., and Wraight, C. A. (2006) Small weak acids reactivate proton transfer in reaction centers from *Rhodobacter sphaeroides* mutated at AspL210 and AspM17. *J. Biol. Chem. 281*, 4413−4422.
(8) Wraight, C. A. (2005) Intraprotein proton transfer: Concepts and realities from the bacterial photosynthetic reaction center. In *Biophysical and Structural Aspects of Bioenergetics* (Wikström, M., Ed.) Chapter 12, pp 273−313, The Royal Society of Chemistry, Cambridge, U.K.
(9) Graige, M. S., Paddock, M. L., Bruce, J. M., Feher, G., and Okamura, M. Y. (1996) Mechanism of proton-coupled electron transfer for quinone (Q_B) reduction in reaction centers of *Rb. sphaeroides*. *J. Am. Chem. Soc. 118*, 9005−9016.
(10) Wraight, C. A. (1979) Electron acceptors of bacterial photosynthetic reaction centers II. H^+ binding coupled to secondary electron transfer in the quinone acceptor complex. *Biochim. Biophys. Acta 548*, 309−327.
(11) Maróti, Á., Wraight, C. A., and Maróti, P. (2015) The rate of second electron transfer to Q_B^- in bacterial reaction center of impaired proton delivery shows hydrogen-isotope effect. *Biochim. Biophys. Acta 1847*, 223−230.
(12) Lonjers, Z. T., Dickson, E. L., Chu, T. P. T., Kreutz, J. E., Neacsu, F. A., Anders, K. R., and Shepherd, J. N. (2012) Identification of a New Gene Required for the Biosynthesis of Rhodoquinone in *Rhodospirillum rubrum*. *J. Bacteriol. 194* (5), 965−971.
(13) Erabi, T., Higuti, T., Kakuno, T., Yamashita, J., Tanaka, M., and Horio, T. (1975) Polarographic studies on ubiquinone-10 and rhodoquinone bound with chromatophores from *Rhodospirillum rubrum*. *J. Biochem. 78* (4), 795−801.
(14) Song, Y., and Buettner, G. R. (2010) Thermodynamic and kinetic considerations for the reaction of semiquinone radicals to form superoxide and hydrogen peroxide. *Free Radical Biol. Med. 49* (6), 919−962.
(15) Graige, M. S., Paddock, M. L., Feher, G., and Okamura, M. Y. (1999) Observation of the protonated semiquinone intermediate in isolated reaction centers from *Rhodobacter sphaeroides*: Implications for the mechanism of electron and proton transfer in proteins. *Biochemistry 38*, 11465−11473.
(16) Wraight, C. A. (1982) The involvement of stable semiquinones in the two-electron gates of plant and bacterial photosystems. In *Function of Quinones in Energy Conserving Systems* (Trumpower, B., Ed.) Chapter 3, pp 59−72, Academic Press, San Diego.
(17) Paddock, M. L., Flores, M., Isaacson, R., Shepherd, J. N., and Okamura, M. Y. (2010) EPR and ENDOR investigation of rhodosemiquinone in bacterial reaction centers formed by B-branch electron transfer. *Appl. Magn. Reson. 37* (1−4), 39−48.
(18) Paddock, M. L., Chang, C., Xu, Q., Abresch, E. C., Axelrod, H. L., Feher, G., and Okamura, M. Y. (2005) Quinone (Q_B) reduction by B-branch electron transfer in mutant bacterial reaction centers from *Rhodobacter sphaeroides*: Quantum efficiency and X-ray structure. *Biochemistry 44*, 6920−6928.
(19) Takahashi, E., Wells, T. A., and Wraight, C. A. (2001) Protein control of the redox potential of the primary acceptor quinone in reaction centers from *Rhodobacter sphaeroides*. *Biochemistry 40*, 1020−1028.
(20) Rinyu, L., Martin, E. W., Takahashi, E., Maróti, P., and Wraight, C. A. (2004) Modulation of the free energy of the primary quinone acceptor (Q_A) in reaction centers from *Rhodobacter sphaeroides*: Contributions from the protein and protein−lipid(cardiolipin) interactions. *Biochim. Biophys. Acta 1655*, 93−101.
(21) Onidas, D., Sipka, G., Asztalos, E., and Maróti, P. (2013) Mutational Control of Bioenergetics of Bacterial Reaction Center Probed by Delayed Fluorescence. *Biochim. Biophys. Acta 1827*, 1191−1199.
(22) Wells, T. A., Takahashi, E., and Wraight, C. A. (2003) Primary Quinone (Q_A) Binding Site of Bacterial Photosynthetic Centers: Mutations at Residue M265 Probed by FTIR Spectroscopy. *Biochemistry 42*, 4064−4074.
(23) Martin, E., Samoilova, R. I., Narasimhulu, K. V., Lin, T. J., O'Malley, P. J., Wraight, C. A., and Dikanov, S. A. (2011) Hydrogen bonding and spin density distribution in the Q_B semiquinone of bacterial reaction centers and comparison with the Q_A site. *J. Am. Chem. Soc. 133* (14), 5525−5537.
(24) Taguchi, A. T., O'Malley, P. J., Wraight, C. A., and Dikanov, S. A. (2013) Conformational differences between the methoxy groups of Q_A and Q_B site ubiquinones in bacterial reaction centers: A key role for methoxy group orientation in modulating ubiquinone redox potential. *Biochemistry 52*, 4648−4655.
(25) Taguchi, A. T., Mattis, A. J., O'Malley, P. J., Dikanov, S. A., and Wraight, C. A. (2013) Tuning Cofactor Redox Potentials: The 2-Methoxy Dihedral Angle Generates a Redox Potential Difference of >160 mV between the Primary (Q_A) and Secondary (Q_B) Quinones of the Bacterial Photosynthetic Reaction Center. *Biochemistry 52*, 7164−7166.
(26) Land, E. J., Simic, M., and Swallow, A. J. (1971) Optical absorption spectrum of half-reduced ubiquinone. *Biochim. Biophys. Acta 226*, 239−240.
(27) Kleinfeld, D., Abresch, E. C., Okamura, M. Y., and Feher, G. (1984) Damping of oscillations in the semiquinone absorption in reaction centers after successive flashes. Determination of the equilibrium between $Q_A^-Q_B$ and $Q_AQ_B^-$. *Biochim. Biophys. Acta 765*, 406−409.
(28) Asztalos, E., Sipka, G., and Maróti, P. (2015) Fluorescence relaxation in intact cells of photosynthetic bacteria: Donor and acceptor side limitations of reopening of the reaction center. *Photosynth. Res.*, DOI: 10.1007/s11120-014-0070-0.
(29) Moore, H. W., and Folkers, K. (1966) Structure of rhodoquinone. *J. Am. Chem. Soc. 88*, 567−570.
(30) Daves, G. D., Wilczynski, J. J., Friis, P., and Folkers, K. (1968) Synthesis of rhodoquinone and other multiprenyl-1,4-benzoquinones biosynthetically related to ubiquinone. *J. Am. Chem. Soc. 90*, 5587−5593.
(31) Giménez-Gallego, G., Ramírez-Ponce, M. P., Lauzurica, P., and Ramírez, J. M. (1982) Photooxidase system of *Rhodospirillum rubrum*. III. The role of rhodoquinone and ubiquinone in the activity preparations of chromatophores and reaction centers. *Eur. J. Biochem. 121*, 343−347.
(32) Okamura, M. Y., Isaacson, R. A., and Feher, G. (1975) Primary acceptor in bacterial photosynthesis: Obligatory role of ubiquinone in photoactive reaction centers of *Rhodopseudomonas sphaeroides*. *Proc. Natl. Acad. Sci. U.S.A. 72*, 3491−3495.
(33) Maróti, P., and Wraight, C. A. (1988) Flash-induced H^+ binding by bacterial photosynthetic reaction centers: Comparison of spectrophotometric and conductimetric methods. *Biochim. Biophys. Acta 934*, 314−328.
(34) Milano, F., Gerencsér, L., Agostiano, A., Nagy, L., Trotta, M., and Maróti, P. (2007) Mechanism of quinol oxidation by ferricenium produced by light excitation in reaction centers of photosynthetic bacteria. *J. Phys. Chem. B 111*, 4261−4270.
(35) Woodbury, N. W., Parson, W. W., Gunner, M. R., Prince, R. C., and Dutton, P. L. (1986) Radical-pair energetics and decay mechanisms in reaction centers containing anthraquinones, naph-

DOI: 10.1021/bi501553t
Biochemistry 2015, 54, 2095−2103

thoquinones or benzoquinones in place of ubiquinone. *Biochim. Biophys. Acta 851*, 6−22.
(36) Shopes, R. J., and Wraight, C. A. (1987) Charge recombination from the $P^+Q_A^-$ state in reaction centers from *Rhodopseudomonas viridis*. *Biochim. Biophys. Acta 893*, 409−425.
(37) Sebban, P. (1988) Activation free energy of $P^+Q_A^-$ absorption decay in reaction centers from *Rb. sphaeroides* reconstituted with different anthraquinones. *FEBS Lett. 233*, 331−334.
(38) Vermeglio, A. (1977) Secondary electron transfer in reaction centers of *Rhodopseudomonas sphaeroides*: Out-of phase periodicity of two for the formation of ubisemiquinone and fully reduced ubiquinone. *Biochim. Biophys. Acta 459*, 516−524.
(39) Stowell, M. H. B., McPhillips, T. M., Rees, D. C., Soltis, S. M., Abresch, E., and Feher, G. (1997) Light-Induced Structural Changes in Photosynthetic Reaction Center: Implications for Mechanism of Electron-Proton Transfer. *Science 276*, 812−816.
(40) Calvo, R., Isaacson, R., Paddock, M. L., Abresch, E. C., Okamura, M. Y., Maniero, A.-L., Brunel, L.-C., and Feher, G. (2001) EPR Study of the Semiquinone Biradical $Q_A^{-\bullet}Q_B^{-\bullet}$ in Photosynthetic Reaction Centers from *Rb. sphaeroides* at 326 GHz: Determination of the Exchange Interaction J_0. *J. Phys. Chem. B 105*, 4053−4057.
(41) Wraight, C. A. (2004) Proton and electron transfer in the acceptor quinone complex of photosynthetic reaction centers from *Rhodobacter sphaeroides*. *Front. Biosci. 9*, 309−337.
(42) Cheap, H., Tandori, J., Derrien, V., Benoit, M., de Oliveira, P., Köpke, J., Lavergne, J., Maróti, P., and Sebban, P. (2007) Evidence for delocalized anticooperative flash induced proton bindings as revealed by mutants at M266His iron ligand in bacterial reaction centers. *Biochemistry 46*, 4510−4521.
(43) Gerencsér, L., Boros, B., Derrien, V., Hanson, D. K., Wraight, C. A., Sebban, P., and Maróti, P. (2015) Stigmatellin probes the electrostatic potential in the Q_B site of photosynthetic reaction center. *Biophys. J. 108*, 379−394.
(44) Rao, P. S., and Hayon, E. (1973) Ionization constants and spectral characteristics of some semiquinone radicals in aqueous solution. *J. Phys. Chem. 77*, 2274−2276.
(45) Willson, R. L. (1971) Semiquinone free radicals: Determination of acid dissociation constants by pulse radiolysis. *J. Chem. Soc. D*, 1249−1250.
(46) Swallow, A. J. (1982) Physical Chemistry of Semiquinones. In *Function of Quinones in Energy Conserving Systems* (Trumpower, B., Ed.) Chapter 3, pp 59−72, Academic Press, San Diego.
(47) Mukherjee, T. (2000) Photo and Radiation Chemistry of Quinones. *PINSA-A: Proc. Indian Natl. Sci. Acad., Part A 66A* (No. 2), 239−265.
(48) Pal, H., Mukherjee, T., and Mittal, J. P. (1994) One-electron reduction of 9,10-anthraquinone, 1-amino-9,10-anthraquinone and 1-hydroxy-9,10-anthraquinone in aqueous isopropanol-acetone mixed solvent: A pulse radiolysis study. *Radiat. Phys. Chem. 44*, 603−609.
(49) Lavergne, J., Matthews, C., and Ginet, N. (1999) Electron and proton transfer on the acceptor side of the reaction center in chromatophores of *Rhodobacter capsulatus*: Evidence for direct protonation of the semiquinone state of Q_B. *Biochemistry 38*, 4542−4552.
(50) Prince, R. C., and Dutton, P. L. (1978) Protonation and the reducing potential of the primary electron acceptor. In *The Photosynthetic Bacteria* (Clayton, R. K., and Sistrom, W. R., Eds.) pp 439−453, Plenum Press, New York.
(51) McPherson, P. H., Nagarajan, V., Parson, W. W., Okamura, M. Y., and Feher, G. (1990) pH-dependence of the free energy gap between DQ_A and $D^+Q_A^-$ determined from delayed fluorescence in reaction centers from *Rhodobacter sphaeroides* R-26. *Biochim. Biophys. Acta 1019*, 91−94.
(52) Turzó, K., Laczkó, G., Filus, Z., and Maróti, P. (2000) Quinone-dependent delayed fluorescence from reaction centers of photosynthetic bacteria. *Biophys. J. 79*, 14−25.
(53) Maróti, P., and Wraight, C. A. (2008) The redox midpoint potential of the primary quinone of reaction centers in chromatophores of *Rhodobacter sphaeroides* is pH independent. *Eur. Biophys. J. 37*, 1207−1217.
(54) Alexov, E., and Gunner, M. R. (1999) Calculated protein and proton motions coupled to electron transfer: Electron transfer from Q_A^- to Q_B in bacterial photosynthetic reaction centers. *Biochemistry 38*, 8254−8270.
(55) McPherson, P. H., Okamura, M. Y., and Feher, G. (1988) Light induced proton uptake by photosynthetic reaction centers from *Rhodobacter sphaeroides* R-26. I. Protonation of the one-electron states $D^+Q_A^-$, DQ_A^-, $D^+Q_AQ_B^-$, and $DQ_AQ_B^-$. *Biochim. Biophys. Acta 934*, 348−368.
(56) McPherson, P. H., Schönfeld, M., Paddock, M. L., Okamura, M. Y., and Feher, G. (1994) Protonation and Free Energy Changes Associated with Formation of Q_BH_2 in Native and Glu-L212 → Gln Mutant Reaction Centers from *Rhodobacter sphaeroides*. *Biochemistry 33*, 1181−1193.
(57) Marcus, R. A., and Sutin, N. (1985) Electron transfers in chemistry and biology. *Biochim. Biophys. Acta 811*, 265−322.
(58) Kleinfeld, D., Okamura, M. Y., and Feher, G. (1985) Electron transfer in reaction centers of *Rhodopseudomonas sphaeroides*. II. Free energy and kinetic relations between the acceptor states $Q_A^-Q_B^-$ and $Q_AQ_B^{2-}$. *Biochim. Biophys. Acta 809*, 291−310.

DOI: 10.1021/bi501553t
Biochemistry 2015, 54, 2095−2103